BUOYANCY DRIVEN FLOW IN A NON-DARCIAN, FLUID-SATURATED POROUS ENCLOSURE SUBJECTED TO UNIFORM HEAT FLUX–A NUMERICAL STUDY

P. NITHIARASU,[1]* K. S. SUJATHA,[2] T. SUNDARARAJAN[3] AND K. N. SEETHARAMU[4]

[1]*Institute for Numerical Methods in Engineering, University of Wales Swansea, Singleton Park, Swansea, SA2 8PP, U.K.*
[2]*Institute of Non-Newtonian Fluid Mechanics, University of Wales Swansea, Singleton Park, Swansea, SA2 8PP, U.K.*
[3]*Department of Mechanical Engineering, Indian Institute of Technology Madras, Chennai, India 600 036*
[4]*School of Mechanical Engineering, Universiti Sains Malaysia, 31750 Tronoh, Malaysia*

SUMMARY

The differences in existing porous medium flow models and their effect on flow and heat transfer are discussed. A fluid-saturated porous medium subjected to constant heat flux has been considered. The Galerkin finite element method coupled with the velocity correction procedure is used to solve a set of generalized porous medium equations. Results are presented for a wide range of Darcy and Rayleigh numbers. Copyright © 1999 John Wiley & Sons, Ltd.

KEY WORDS   generalized porous medium model; heat flux boundary condition; semi-implicit scheme; finite element method

1. INTRODUCTION

Porous applications such as thermal insulation, alloy solidification, etc. need an appropriate flow model along with thermal wall conditions different from constant temperature. For instance, the generalized porous medium flow model combined with either uniform heat flux condition on a wall or heat transfer coefficient and atmospheric temperature conditions is such an example. In this study, we consider such a problem for a detailed analysis and the problem is the buoyancy driven flow in a non-Darcy porous medium subjected to constant heat flux condition. This basic study on porous flow and heat transfer is intended to understand the differences encountered by different porous medium flow models in the context of heat flux boundary condition. Also, in the present study, results are presented for a wide range of Darcy and Rayleigh numbers using the full generalized porous medium equations. These equations are appropriately modified to isolate the effects of non-linear drag term and porosity. The present predictions are compared with the existing Brinkman and Darcy results.

Only a few studies have been reported in the literature with uniform wall heat flux conditions. Prasad and Kulacki[1] analysed the natural convection in a rectangular cavity and the effects of aspect ratio on heat transfer and flow structure. Natural convection in a vertical porous annulus with constant heat flux on the inner wall has been studied numerically by Prasad.[2] These studies are based on the Darcy flow model, which is applicable only when the porosity and the Rayleigh

---

*Correspondence to: P. Nithiarasu, Department of Civil Engineering, University of Wales Swansea, Singleton Park, Swansea SA2 8PP, U.K.

number are small. Recently Satya Sai *et al.*[3] used the Brinkman extended Darcy model with advection terms to study this problem. Again the model is not general enough to account for the effects of porosity and non-linear drag. Thus, we need further investigation of this problem to bring out the influence of these ignored parts on flow and heat transfer.

Some studies have used the generalized porous medium model in the past[4–8] to study either forced convection through packed-beds or to investigate the constant wall temperature condition. However, no detailed analysis is available for buoyancy driven flow in a non-Darcian porous medium subjected to the uniform wall heat flux condition using the generalized porous medium approach. Few recent articles[3,9] use a model which ignores the porosity and/or non-linear drag effects. Available studies using the generalized model (derived from first principles) with iso-thermal wall conditions indicate that the contribution from these ignored parts of the model can be significant for different parameter variation.[7,10,11] These two effects are important when the flow is no longer in the Darcy flow regime (i.e. for $Da\,10^{-4}$). If we consider a general application such as alloy solidification,[12] flow over heat exchanger tubes,[13] etc., the Darcy number can vary from zero to infinity. In such conditions if the Rayleigh number is also high, the inclusion of porosity and non-linear effects are essential to predict accurate flow and heat transfer results. In this paper, in addition to a demonstration on the effects of previously ignored parts, we also present results for a wide range or Darcy and Rayleigh numbers for the first time using the generalized porous medium flow model. A powerful semi-implicit type of time marching coupled with the Galerkin finite element discretization is employed to solve the porous medium equations.

2. PROBLEM FORMULATION AND GOVERNING EQUATIONS

A square cavity filled with a fluid saturated porous medium having insulated horizontal walls and one of the vertical walls subjected to constant uniform heat flux and the other with an isothermal condition is considered (Figure 1). The velocity components are assumed to be equal to zero on
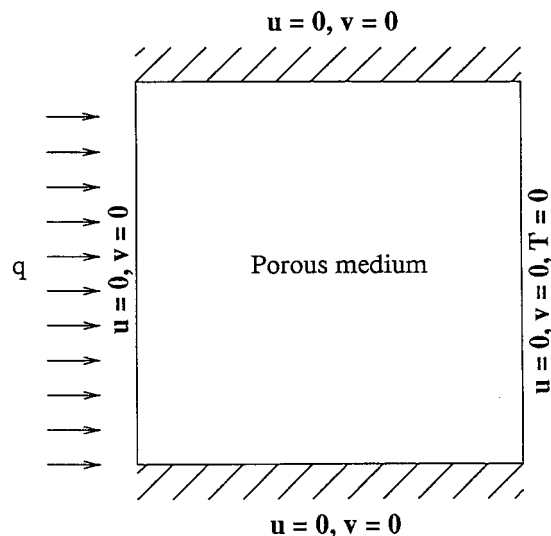

Figure 1. Buoyancy driven flow in porous cavity subjected to constant heat flux

all walls. The properties except the density are assumed to be constant and the density variation is incorporated through Boussinesq approximation. The generalized set of non-dimensional governing equations for the natural convective flow and heat transfer with uniform porosity are given as follows:

Continuity equation

$$\frac{\partial u}{\partial x} + \frac{\partial v}{\partial y} = 0 \tag{1}$$

x-momentum equation

$$\frac{1}{\varepsilon}\frac{\partial u}{\partial t} + \frac{1}{\varepsilon^2}u\frac{\partial u}{\partial x} + \frac{1}{\varepsilon^2}v\frac{\partial u}{\partial y} = -\frac{\partial p}{\partial x} + \frac{J\mathrm{Pr}}{\varepsilon}\left[\frac{\partial^2 u}{\partial x^2} + \frac{\partial^2 u}{\partial y^2}\right] - \frac{\mathrm{Pr}}{\mathrm{Da}}u - \frac{1 \cdot 75}{\sqrt{150}}\frac{|\bar{V}|}{\sqrt{\mathrm{Da}}}\frac{u}{\varepsilon^{3/2}} \tag{2}$$

y-momentum equation

$$\frac{1}{\varepsilon}\frac{\partial v}{\partial t} + \frac{1}{\varepsilon^2}u\frac{\partial v}{\partial x} + \frac{1}{\varepsilon^2}v\frac{\partial v}{\partial y} = -\frac{\partial p}{\partial y} + \frac{J\mathrm{Pr}}{\varepsilon}\left[\frac{\partial^2 v}{\partial x^2} + \frac{\partial^2 v}{\partial y^2}\right] - \frac{\mathrm{Pr}}{\mathrm{Da}}v - \frac{1 \cdot 75}{\sqrt{150}}\frac{|\bar{V}|}{\sqrt{\mathrm{Da}}}\frac{u}{\varepsilon^{3/2}} + \mathrm{RaPr}T \tag{3}$$

Energy equation

$$\sigma\frac{\partial T}{\partial t} + u\frac{\partial T}{\partial x} + v\frac{\partial T}{\partial y} = k*\left(\frac{\partial^2 T}{\partial x^2} + \frac{\partial^2 T}{\partial y^2}\right) \tag{4}$$

The detailed derivation of the governing equations is discussed elsewhere.[7] In the momentum equations (2, 3), the non-linear matrix drag is incorporated through Ergun's correlation;[14] u and v are volume-averaged velocity components; ε is the porosity of the medium and is assumed to be uniform throughout the domain; Pr is the Prandtl number, Ra is the fluid Rayleigh number, Da is the Darcy number, σ is the ratio of heat capacities and T is the non-dimensional temperature.

In the momentum equations (2, 3), J is the viscosity ratio. This ratio and the conductivity ratio $k*$ in the energy equation are taken as unity in the present study for the sake of simplicity. It is also assumed that the thermal equilibrium between the phases exists. The advection terms are also included to entertain porosity values from 0 to 1.[7] Even though the contribution of this term is small for a porous medium flow, it is included in the model to handle all possible situations including the single phase fluid. Also, from Reference 4 it is clear that, for the development of the boundary layer, it is necessary to include the advection terms.

The near wall porosity variation is not considered in the present study. This has already been investigated by different authors in the past.[7,15] In applications such as thermal insulation systems, either the solid particle size is small or it is a kind of matrix. The near wall porosity variations in such applications are negligibly small and can be neglected. Near wall variation in porosity significantly affects the heat transfer only when the ratio of solid particle size to the characteristics dimension of the cavity is high. This is true when the porous medium is made up of regularly shaped particles such as packed beds.

2.1. Thermal boundary condition

In the porous cavity considered (Figure 1), the left side wall is assumed to be at uniform constant heat flux and the right side wall is assumed to be at a constant temperature. Both the horizontal walls are assumed to be insulated. The temperature scale employed is

$$T = \frac{\bar{T} - T_{\mathrm{c}}}{\dfrac{qL}{k_{\mathrm{f}}}} \tag{5}$$

and the fluid Rayleigh number is defined as

$$\mathrm{Ra} = \frac{g\beta qL^4}{k_{\mathrm{f}}\nu_{\mathrm{f}}\alpha_{\mathrm{f}}} \tag{6}$$

where q is the applied heat flux, L the characteristic dimension, k_{f} the thermal conductivity of the fluid, g the acceleration due to gravity, β the coefficient of thermal expansion, ν_{f} the fluid kinematic viscosity and α_{f} the fluid thermal diffusivity. The average Nusselt number is calculated from the relation

$$\mathrm{Nu} = \frac{1}{\displaystyle\int_0^1 (T_{\mathrm{w}} - T_{\mathrm{c}})\,\mathrm{d}l} \tag{7}$$

Other non-dimensional parameters used in the study are:

$$
\begin{aligned}
x &= \frac{\bar{x}}{L}, \quad y = \frac{\bar{y}}{L}, \quad u = \frac{\bar{u}L}{\alpha_{\mathrm{f}}}, \quad v = \frac{\bar{v}L}{\alpha_{\mathrm{f}}} \\
p &= \frac{\bar{p}\alpha_{\mathrm{f}}}{\rho L^2}, \quad t = \frac{\bar{t}\alpha_{\mathrm{f}}}{L^2}, \quad k^* = \frac{k}{k_{\mathrm{f}}} \\
\alpha_{\mathrm{f}} &= \frac{k_{\mathrm{f}}}{(\rho c_p)_{\mathrm{f}}}, \quad \mathrm{Pr} = \frac{\nu_{\mathrm{f}}}{\alpha_{\mathrm{f}}}, \quad \mathrm{Da} = \frac{\kappa}{L^2}
\end{aligned}
\tag{8}
$$

where the over-bar indicates a dimensional quantity.

3. SOLUTION PROCEDURE

In the present study, the Galerkin finite element method coupled with the Eulerian velocity correction procedure is used. The semi-implicit type of time marching is adopted to accelerate convergence.[16] The split algorithm (also called velocity correction or projection method) was originally introduced by Chorin[17] in the finite difference context. Later it was extended to finite elements by many authors. This algorithm, coupled with the semi-implicit type of time discretization, has been used by Ramaswamy *et al.*[16] to study single-phase fluid flow. The comparative study by the authors between the explicit method and the semi-implicit method favoured the latter due to its smaller CPU time consumption. In the present study, the generalised porous medium equations are solved using the semi-implicit type of time marching.

The velocity correction procedure is well established and available in many research articles. Four essential steps in the scheme can be briefly stated as:

1. solving the momentum equations without pressure terms
2. calculation of pressure from the Poisson equation
3. correcting the velocities
4. calculation of the temperature field from the energy equation.

The main advantage of using the velocity correction procedure is due to equal order interpolation for pressure and velocity which reduces the complexity and CPU time. From step 1, the intermediate vertical velocity component is calculated as

$$
\frac{\tilde{v}^{n+1} - v^n}{\varepsilon \Delta t} = -\frac{3}{2\varepsilon^2}\left[u\frac{\partial v}{\partial x} + v\frac{\partial v}{\partial y}\right]^n + \frac{1}{2\varepsilon^1}\left[u\frac{\partial v}{\partial x} + v\frac{\partial v}{\partial y}\right]^{n-1}
$$
$$
+ \left[\frac{\mathrm{Pr}J}{\varepsilon}\left(\frac{\partial^2 \tilde{v}}{\partial x^2} + \frac{\partial^2 \tilde{v}}{\partial y^2}\right) - \frac{\mathrm{Pr}}{\mathrm{Da}}\tilde{v} - \frac{1{\cdot}75}{\sqrt{150}}\frac{|\bar{V}|}{\sqrt{\mathrm{Da}}}\frac{\tilde{v}}{\varepsilon^{3/2}}\right]^{n+1} + \mathrm{RaPr}T^n \tag{9}
$$

where 'tilde' indicates the intermediate velocity component. Here, the porous medium terms are treated implicitly in addition to the viscous terms. This is necessary as these terms impose a heavy restriction on the time step if they are treated explicitly. The Galerkin finite element method is used for the spatial discretization of the above equation. The final matrix form of the discretized equation is given as

$$
\{[M] + \Delta t[K] + \Delta t[D_1] + \Delta t[D_2]\}\tilde{v} = [M]v^n + \Delta t\{\{F\} - [A_1]v^n + [A_2]v^{n-1}\} + \Delta t[G]T^n \tag{10}
$$

where $\{F\}$ is the boundary term from the viscous contribution,

$$
[M] = \frac{1}{\varepsilon}\int_\Omega N^{\mathrm{T}}N\,\mathrm{d}\Omega \tag{11}
$$

$$
[K] = \frac{J\mathrm{Pr}}{\varepsilon}\int_\Omega \frac{\partial N^{\mathrm{T}}}{\partial x_i}\frac{\partial N}{\partial x_i}\,\mathrm{d}\Omega \tag{12}
$$

$$
[D_1] = \frac{\mathrm{Pr}}{\mathrm{Da}}\int_\Omega N^{\mathrm{T}}N\,\mathrm{d}\Omega \tag{13}
$$

$$
[D_2] = \frac{1{\cdot}75}{\sqrt{150}}\frac{\sqrt{(u^2 + v^2)}^n}{\sqrt{\mathrm{Da}}}\frac{1}{\varepsilon^{3/2}}\int_\Omega N^{\mathrm{T}}N\,\mathrm{d}\Omega \tag{14}
$$

$$
[A_1] = \frac{1}{\varepsilon^2}\left[\frac{3}{2}\int_\Omega N^{\mathrm{T}}Nu_j^n\frac{\partial N^{\mathrm{T}}}{\partial x_j}\,\mathrm{d}\Omega\right] \tag{15}
$$

$$
[A_2] = \frac{1}{\varepsilon^2}\left[\frac{1}{2}\int_\Omega N^{\mathrm{T}}Nu_j^{n-1}\frac{\partial N^{\mathrm{T}}}{\partial x_j}\,\mathrm{d}\Omega\right] \tag{16}
$$

$$
[G] = \mathrm{RaPr}\int_\Omega N^{\mathrm{T}}N\,\mathrm{d}\Omega \tag{17}
$$

Integration of the above quantities for linear triangular elements is simple, and is discussed in many textbooks.[18]

The time marching of the four steps is continued until the nodal velocities, pressure and temperature approach steady state within a specified difference in the value of the variable between successive time-steps. The maximum tolerance (residual) value has been set as 10^{-7} for velocity and temperature fields, and 10^{-5} for pressure.

4. RESULTS AND DISCUSSION

In order to prove the suitability of the finite element mesh used, a mesh sensitivity study is carried out first. In Table I, the results of this study are presented for the highest Darcy and Rayleigh numbers considered in this paper. The difference between the Nusselt number values of 51×51 and 61×61 meshes is less than 0·5%, and between 41×41 and 51×51 meshes the difference is about 0·8%. In these meshes, the first point from the walls is placed at a distance of 0·008, 0·005 and 0·003, respectively, for the meshes 41×41, 51×51 and 61×61. The remaining part of the domain is discretized using a structured grid by geometric progression from the walls towards the centre of the cavity with small elements near walls. If we assume that the results from the mesh 61×61 are equivalent to exact, then the errors in Nusselt number from 41×41 and 51×51 meshes are under 1%. Since the sensitivity study is carried out for the highest Rayleigh and Darcy numbers, the error in the other results will definitely be less than 1%. Neglecting the minor differences between the 61×61 and 51×51 meshes and considering the advantage of smaller CPU time, a 51×51 mesh is definitely a better choice than the 61×61 mesh. Thus, in the present study, a 51×51 size mesh has been employed for all calculations.

Table I. Grid sensitivity study, $Da = 10^{-3}$ $Ra = 10^{9}$, $\varepsilon = 0.6$, $Pr = 1.0$

Sl. no.	Parameters	41×41	51×51	61×61
1	Nu	21·203	21·370	21·431
2	$\|v_{max}\|$	789·588	802·314	812·622
3	$\|\psi_{max}\|$	26·325	26·647	26·772

For validation purposes, the present predictions in the Darcy flow regime are compared with the existing results for a square cavity subjected to constant wall heat flux conditions, and the comparison is shown in Figure 2. Here the general porous medium model is solved in the Darcy flow regime with a small Darcy number ($Da = 10^{-6}$) to match the existing Darcy regime results. Overall, the agreement with the existing results is seen to be good for all Darcy–Rayleigh numbers ($Ra^* = RaDa$) considered. Small differences can be attributed to the different models used by the existing studies. More experimental and analytical comparisons are available for constant wall temperature conditions in our earlier publications.[7,10]

Table II shows the comparison of the present average Nusselt number predictions with the results available in the literature for the same problem. The cited paper[3] uses the Brinkman extended Darcy model with extra advection terms. In the present study, the Nusselt number is also a function of bed porosity in addition to the usual parameters, Darcy, Rayleigh and Prandtl numbers, and geometry. It has been proved that the porosity significantly affects the Nusselt number prediction at higher Darcy and Rayleigh numbers.[11] The porosity effect has not

Table II. Comparison of present average Nusselt number predictions with the existing results

Sl. no.	Da	Ra	Ref. 3	Darcy[1]	Present $\varepsilon = 1$, Pr = 0·72 with non-linear drag	Present $\varepsilon = 1$, Pr = 0·72 without non-linear drag
1	10^{-6}	10^8	2·100	2·250	2·109	2·111
2	10^{-5}	10^7	2·100	2·250	2·086	2·091
3	10^{-4}	10^6	2·050	2·250	2·004	2·018
4	10^{-3}	10^5	1·900	2·250	1·819	1·843
5	10^{-6}	10^9	5·400	6·000	5·380	5·400
6	10^{-5}	10^8	5·200	6·000	5·222	5·262
7	10^{-4}	10^7	4·850	6·000	4·743	4·848
8	10^{-3}	10^6	4·000	6·000	3·931	4·069

been accounted for in the cited paper.[13] Also, the non-linear effects are not considered in this work. In the present study, the porous medium model used is capable of taking into account the above-mentioned effects. Table II shows the effects of non-linear drag and porosity on Nusselt number at lower Darcy–Rayleigh number ranges (up to Ra* = 1000). Here, to match the existing results, the Prandtl number is taken equal to 0·72 and $\varepsilon = 1·0$. The results show that the non-linear effects are only small on the heat transfer in this lower Rayleigh number range. Earlier studies suggest that the non-linear drag and porosity effects are high at higher Darcy and Rayleigh numbers, which is investigated in the following paragraph.

To demonstrate the non-linear drag and porosity effects, more results are presented in Tables III and IV at higher Darcy and Rayleigh numbers. Here, the average Nusselt number, magnitudes of maximum vertical velocity component and streamfunction are compared for two different porosity values and the model with and without the non-linear matrix drag term. A maximum difference of about 7% in average Nusselt number, 16% in maximum vertical
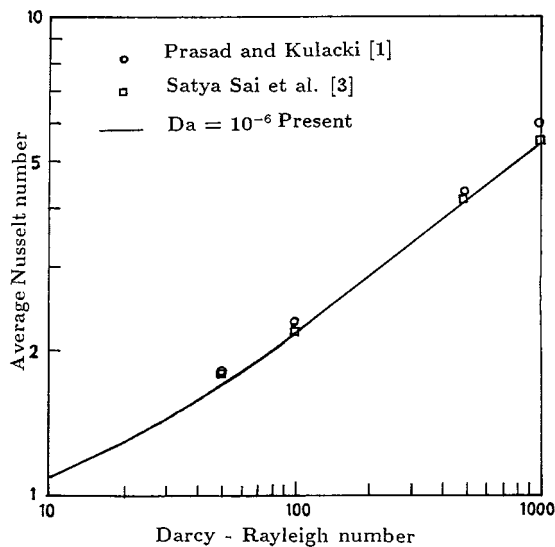

Figure 2. Comparison of present predictions with the available theoretical results

Table III. Comparison of average Nusselt number predictions with and without non-linear drag at higher Rayleigh numbers, Da $= 10^{-3}$

Sl. no.	Ra	ε	With non-linear drag	Without non-linear drag
1	10^7	0·6	7·049	7·551
2	10^8	0·6	12·657	13·570
3	10^9	0·6	21·370	22·933
4	10^7	0·9	7·705	8·076
5	10^8	0·9	13·906	14·749
6	10^9	0·9	23·457	23·017

Table IV. Comparison of velocity and streamfunction values with and without non-linear drag at higher Rayleigh numbers, Da $= 10^{-3}$

Sl. no.	Ra	ε	$\lvert v_{max}\rvert$ with non-linear drag	$\lvert v_{max}\rvert$ without non-linear drag	$\lvert \psi_{max}\rvert$ with non-linear drag	$\lvert \psi_{max}\rvert$ without non-linear drag
1	10^7	0.6	123.981	144.145	10.169	11.028
2	10^8	0.6	358.696	379.440	18.040	18.902
3	10^9	0.6	809.314	962.560	26.647	30.881
4	10^7	0.9	156.880	168.138	11.225	11.769
5	10^8	0.9	392.773	435.052	18.444	20.227
6	10^9	0.9	970.417	1101.340	29.389	33.288

velocity component and 14% in streamfunction is observed between the results with and without the non-linear drag. The effects of increase in porosity from 0·6 and 0·9 can be clearly seen from the increase in Nusselt number, vertical velocity and streamfunction as shown in Tables III and IV. A maximum increase of about 9% in Nusselt number, 15% in vertical velocity and about 9·5% in streamfunction are observed. This has proved that the effects of porosity and non-linear drag term are significant at higher Darcy and Rayleigh numbers. Therefore it is essential to include these effects when modelling the porous medium flow in the non-Darcy regime with higher Rayleigh numbers.

Figure 3 shows the flow and isothermal patterns at different Rayleigh and Darcy numbers. Flow and isothermal patterns at Da $= 10^{-7}$ are similar to the patterns observed using Darcy flow models.[1] However, the flow and isotherms at a Darcy number 10^{-3} show an entirely different structure. Unlike in the Darcy flow regime, the results presented for Da $= 10^{-3}$ are very strongly in the boundary layer flow regime with strong convective channelling near the hot and cold walls at a Rayleigh number of 10^9. This is expected because the medium considered at Da $= 10^{-3}$ is highly permeable and thus has strong convective motion. Both in the Darcy and non-Darcy flow regimes, the heat transfer is observed to be away from the diffusion mode at higher Rayleigh numbers. However, heavy convective channelling effects are not observed in the Darcy flow regime with small Darcy numbers as the medium is less permeable in nature. More discussion on the flow and isothermal patterns is given in the following paragraph along with Nusselt number distribution.

Figure 4 shows the average Nusselt number variation with Rayleigh number for different Darcy numbers. It is observed that the convective mode of heat transfer is delayed as the Darcy number decreases. At higher Darcy numbers, the well established conduction, asymptotic and boundary layer heat transfer regimes[1] are observed for the Rayleigh number range considered.
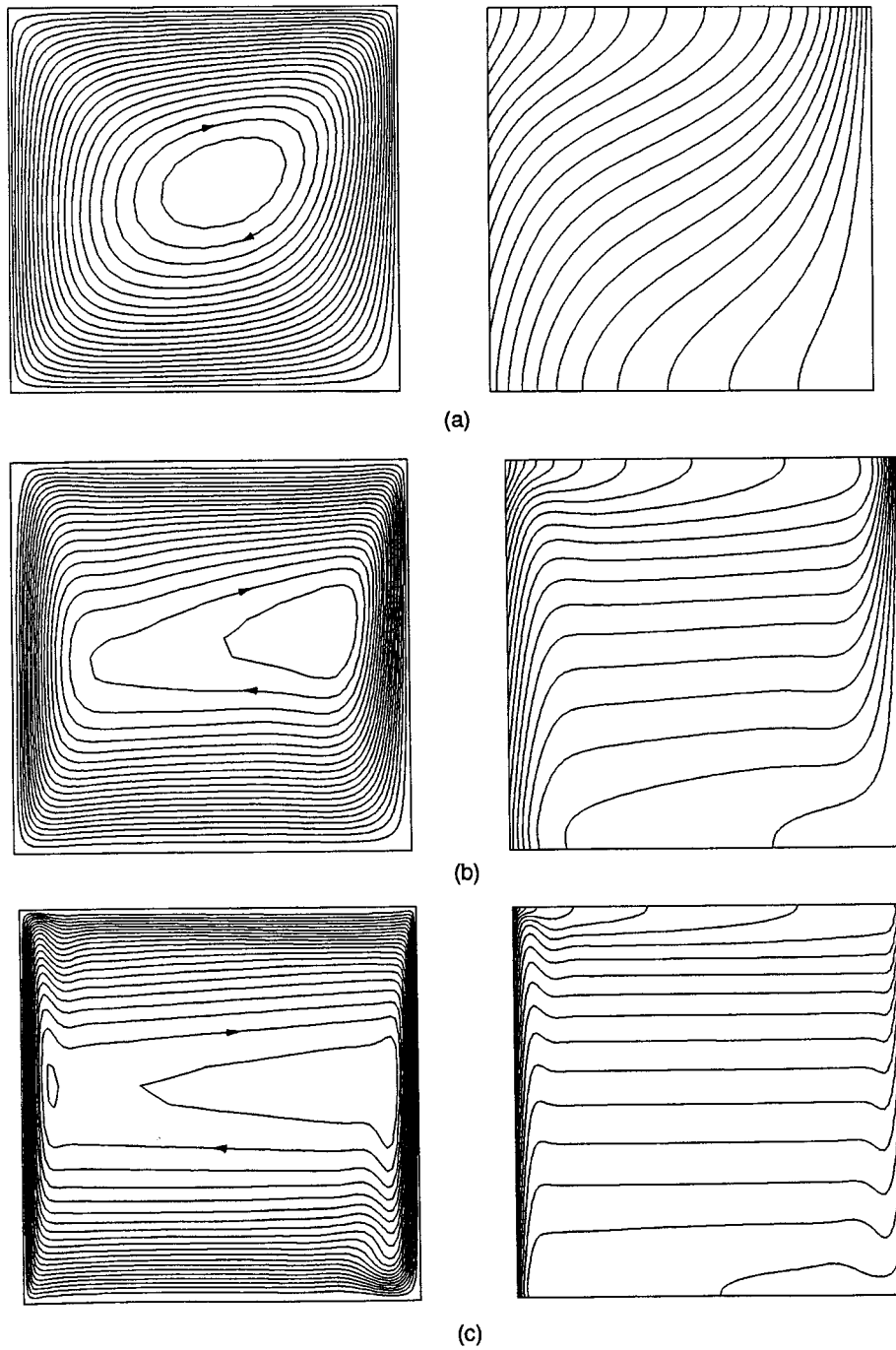
Figure 3. Flow and isothermal patterns for a porous cavity subjected to constant heat flux: (a) $Da = 10^{-7}$, $Ra = 10^9$, $\psi_{max} = 2.541$, $\psi_{min} = 0.0$, $T_{max} = 0.666$; (b) $Da = 10^{-3}$, $Ra = 10^8$, $\psi_{max} = 18.04$, $\psi_{min} = -0.144$, $T_{max} = 0.134$; (c) $Da = 10^{-3}$, $Ra = 10^9$, $\psi_{max} = 26.647$, $\psi_{min} = -0.0114$, $T_{max} = 0.0832$
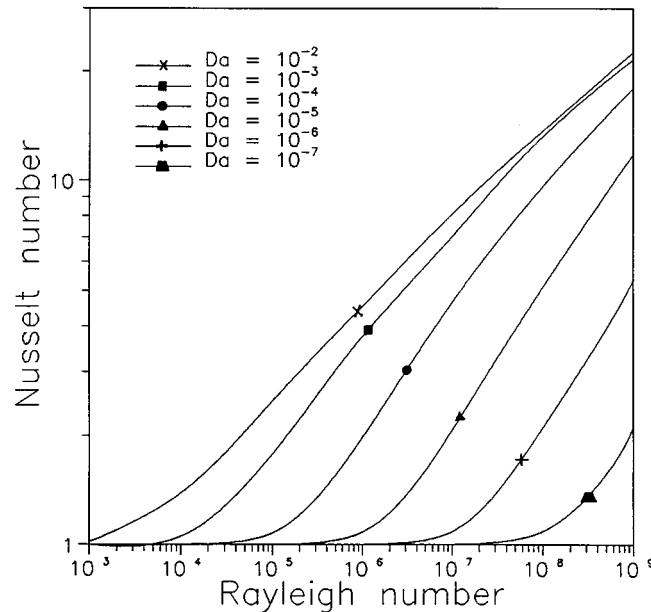
Figure 4. Average Nusselt number variation with Rayleigh number for different Darcy numbers

The conduction regime is the range where the diffusion dominates and slopes of the Nusselt number curves are nearly equal to zero (Nu is almost constant). This regime occurs at a lower Rayleigh number range where heat transfer is mainly by direct diffusion from hot wall to cold wall. In the asymptotic regime, which follows the conduction regime, the mode is changed from pure conduction and heat is transferred across the vertical walls of the cavity by both convection and diffusion. For example, consider Figure 3(a), where the temperature gradient exists even in the middle of the cavity to transfer the heat by diffusion in the horizontal direction and convective motion of the fluid with a thick boundary layer aids the diffusion in transferring more energy. Thus in this mode the rate of heat transfer is higher than that of other two regimes. In the third regime, Figure 3(c), the convective motion of the fluid with thin boundary layers is the major source of energy transfer. Here, the temperature gradient at the centre of the cavity, in the horizontal direction, is nearly zero. Thus the changeover from the asymptotic regime to the boundary layer regime leads to a decrease in the rate of energy transfer. All these regimes are visible in the Nusselt number curves presented in Figure 4. The conduction regime is seen to have almost zero slope followed by an asymptotic regime with a steep increase and the boundary layer regime (only at higher Darcy numbers) with a decreasing slope. Another physical phenomenon inferred from the Nusselt number distribution at higher Darcy and Rayleigh numbers is that the problem approaches a single phase flow case as the Darcy number approaches higher values. This is especially clear from Nusselt number distribution at higher Darcy numbers where the Nu values approach each other as Da increases. This is more clearly seen at higher Rayleigh numbers due to the logarithmic scale used in this Figure. In the Darcy flow regime ($Da < 10^{-5}$), the boundary layer type of flow has not been observed for the Rayleigh number range considered. Here, at lower Darcy numbers, a longer conduction regime followed by an asymptotic flow are observed. This is due to the more packed nature of the medium at lower Darcy numbers.

5. CONCLUSIONS

Natural convective flow and heat transfer through a porous medium subjected to constant heat flux have been studied using the finite element method. The non-Darcian effects, the non-linear drag and porosity, on heat transfer and flow, are demonstrated and their influences at higher Darcy and Rayleigh numbers are determined quantitatively. The differences between the Darcy and non-Darcy flow regimes are brought out through a parametric study using the complete generalized flow model. Different heat transfer modes are observed in the Darcy and Rayleigh number ranges considered. While the non-Darcy regime at higher Darcy numbers is dominated by all three heat transfer regimes at different Rayleigh number ranges, the Darcy regime considered has had only conduction and asymptotic regimes. Further investigation at higher Rayleigh numbers in the Darcy regime can give more information on the heat transfer characteristics. With increasing Darcy numbers the flow approaches a single phase system where the difference in Nusselt number values between different Darcy numbers is small. Although the present study has given a clear basic understanding of the generalized porous flow in a square cavity, further study is needed to understand a wide spectrum of problems. For example, axisymmetric geometries, geometries with higher aspect ratios and application of the approach to practical problems such as thermal insulation, solidification, etc. are subjects for future research.

APPENDIX. NOMENCLATURE

c_p specific heat
Da   Darcy number
g acceleration due to gravity
J viscosity ratio ($\mu_{\text{eff}}/\mu_{\text{f}}$)
k average thermal conductivity ($\varepsilon k_{\text{f}} + (1 - \varepsilon)k_{\text{s}}$)
k^* conductivity ratio
L characteristic dimension
l local length
N shape functions
Nu   average Nusselt number
p pressure
Pr   Prandtl number
q heat flux
Ra   Rayleigh number
Ra*   Darcy–Rayleigh number (Ra Da)
T temperature
t time
$|\bar{V}|$ magnitude of velocity vector ($\sqrt{u^2 + v^2}$)
u, v velocity components
x, y co-ordinate axes

Subscripts

c   cold
f   fluid
eff   effective

h   hot
s   solid
w   wall

Greek Symbols

α thermal diffusivity
β coefficient of thermal expansion
ε porosity
κ permeability
ν kinematic viscosity
σ ratio of heat capacities, $(\varepsilon(\rho c_p)_f + (1 - \varepsilon(\rho c_p)_s)/(\rho c_p)_f$
ρ density

REFERENCES

1. V. Prasad and F. A. Kulacki, 'Natural convection in a rectangular porous cavity with constant heat flux in one vertical wall', *ASME J. Heat Transf.*, **106**, 152–157 (1984).
2. V. Prasad, 'Numerical study of natural convection in a vertical porous annulus with constant heat flux on the inner wall', *Int. J. Heat Mass Transf.*, **29**, 841–853 (1986).
3. Satya B. V. K. Sai, K. N. Seetharamu and P. A. Aswathanarayana, 'Finite element analysis of heat transfer by natural convection in vertical enclosures: Investigations in Darcy and non-Darcy regimes', *Int. J. Numer. Methods Heat Fluid Flow*, **7**, 367–401 (1997).
4. D. Nield, K. Vafai and S. H. Kim, 'Closure statements on the Brinkman–Forchheimer-extended Darcy model', *Int. J. Heat Fluid Flow*, **17**, 34–35 (1996).
5. K. Vafai and C. L. Tien, 'Boundary and inertia effects on flow and heat transfer in porous media', *Int. J. Heat Mass Trans.*, **24**, 195–203 (1981).
6. C. T. Hsu and P. Cheng, 'Thermal dispersion in a porous medium', *Int. J. Heat Mass Transf.*, **33**, 1587–1597 (1990).
7. P. Nithiarasu, K. N. Seetharamu and T. Sundararajan, 'Natural convective heat transfer in an enclosure filled with fluid saturated variable porosity medium', *Int. J. Heat Mass Transf.*, **40**(16), 3955–3967 (1997).
8. J. L. Lage, 'On theoretical prediction of transient heat transfer within a rectangular fluid saturated porous media', *ASME J. Heat Transf.*, **115**, 1069–1071 (1993).
9. D. Misra and A. Sarkar, 'A comparative study of porous media models in a differentially heated square cavity using finite element method', *Int. J. Numer. Methods Heat Fluid Flow*, **16**, 735–752 (1995).
10. P. Nithiarasu, K. N. Seetharamu and T. Sundararajan, 'Double-diffusive natural convection in an enclosure filled with fluid saturated porous medium – A generalised non-Darcy approach', *Numer. Heat Transf. A, Appl.*, **30**, 413–426 (1996).
11. P. Nithiarasu, K. N. Seetharamu and T. Sundararajan, 'Effects of porosity on natural convective heat transfer in a fluid saturated porous medium', *Int. J. Heat Fluid Flow*, **19**, 56–58 (1998).
12. S. K. Sinha, T. Sundararajan and V. K. Garg, 'A variable property analysis of alloy solidification using the anisotropic porous medium approach', *Int. J. Heat Mass Transf.*, **35**, 2865–2877 (1992).
13. A. R. Chaudhuri, K. N. Seetharamu and T. Sundararajan, 'Modelling of steam surface condenser using finite element method', *Commun. Numer. Methods Eng.*, **13**, 909–921 (1997).
14. S. Ergun, 'Fluid flow through packed column', *Chem. Eng. Prog.*, **48**, 89–94 (1952).
15. E. David, G. Lauriat and P. Cheng, 'A numerical solution of variable porosity effects on natural convection in a packed sphere cavity', *ASME J. Heat Transf.*, **113**, 391–399 (1991).
16. B. Ramaswamy, T. C. Jue and J. E. Akin, 'Semi-implicit and explicit finite element schemes for coupled fluid/thermal problems', *Int. J. Numer. Methods Eng.*, **34**, 675–696 (1992).
17. A. J. Chorin, 'Numerical solution of Navier Stokes equations', *Math. Comput.*, **22**, 745–762 (1968).
18. O. C. Zienkiewicz and R. L. Taylor, *The Finite Element Method, Basic Formulations and Linear Problems*, Vol. 1, McGraw Hill International Editions, 1989.